Charge-transfer variation caused by symmetry breaking in a mixed-stack organic compound: TTF-2, $5Cl_2BQ$

1999 J. Phys.: Condens. Matter 11 4163

(http://iopscience.iop.org/0953-8984/11/21/305)

J. Phys.: Condens. Matter **11** (1999) 4163–4177. Printed in the UK PII: S0953-8984(99)96347-6

Charge-transfer variation caused by symmetry breaking in a mixed-stack organic compound: TTF-2, $5Cl_2BQ$

C Katan and C Koenig

Groupe Matière Condensée et Matériaux‡, Université Rennes-1, 35042 Rennes-Cédex, France

E-mail: claudine.katan@univ-rennes1.fr

Received 29 July 1998, in final form 23 December 1998

Abstract. In the 'neutral-to-ionic' transition presented by some mixed-stack organic compounds, the inter-molecular charge-transfer variation at the critical pressure or temperature results both from the loss of inversion symmetry and the lattice contraction. We present here a three-dimensional *ab initio* study of the electronic ground state of one of these charge-transfer salts: tetrathiafulvalene-2, 5-dichloro-p-benzoquinone, and discuss the relative importance of the intra- and inter-chain quantum interactions. Within a tight-binding scheme fitted to the self-consistent results, we show that the weak molecular distortions due to the symmetry-breaking part of the 'neutral-to-ionic' transformation induce a non-negligible contribution to the total charge-transfer variation.

1. Introduction

In the last 20 years, a new class of organic charge-transfer salts has emerged, which are formed by mixed stacks of alternating donor (D) and acceptor (A) molecules. Their very unusual behaviour under pressure or temperature variations results both from the molecular character of the elementary entities and from the nearly one-dimensional (1D) character of several of their physical properties. In some of these compounds, a structural phase transition occurs, where the loss of inversion symmetry is accompanied by a large charge-transfer (CT) variation $\Delta\rho$ from the donor to the acceptor molecule, leading to what has been called the neutral-to-ionic (N–I) transition [1, 2].

Monoclinic tetrathiafulvalene-chloranil (or TTF-CA) is the prototype salt showing this N–I transition. At normal pressure, its ferroelectric transition at a critical temperature of about 80 K is characterized by a CT discontinuity [2] of about $0.4e^-$, a discontinuous lattice contraction and a small distortion (or pairing) of the D and A molecules [3]. The influence of pressure on this CT has been extensively studied. It has in particular been shown that at high pressure the transition line must split into two lines: an isostructural one (lattice contraction) and another one associated with the symmetry breaking (loss of inversion symmetry) [4]. When replacing two equivalent Cl atoms in the CA molecule by two H atoms, one gets the 2, 5-dichloro-p-benzoquinone (or 2, $5Cl_2BQ$) molecule, which, combined with TTF, forms the mixed-stack TTF-2, $5Cl_2BQ$ compound. This compound has been reported to present a continuous N–I transition: at room temperature, its CT varies from $\rho \simeq 0.2e^-$ in the neutral state at atmospheric pressure to $\rho \simeq 0.8e^-$ at high pressure, with no discontinuity at the critical pressure $P_c \simeq 4$ GPa [5]. No transition has been observed under temperature decrease at

‡ UMR au CNRS 6626.

0953-8984/99/214163+15$19.50

atmospheric pressure. Monoclinic tetramethylbenzidine-tetracyanoquinodimethane (or TMB-TCNQ) has also been classified in this category, though in this compound the CT variation is much smaller [6]: $\Delta\rho \simeq 0.1e^-$. A more complicated transition occurs on cooling in dimethyl-TTF-CA (or DMTTF-CA), from a neutral ($\rho \simeq 0.2e^-$) to a N–I coexistence phase ($\rho_N \simeq 0.3e^-$ and $\rho_I \simeq 0.6e^-$), with possible formation of a staging superlattice [7]. These examples show the diversity of the N–I transition. In all these crystals, a strong anisotropy has been observed in the electric and optical properties [8]. There are however indications that the three-dimensional aspects (namely the different chain configurations and corresponding inter-chain interactions) may be partly responsible for the different features of the phase transition.

Phenomenological theories based on 1D Hubbard-like Hamiltonians [9] or free-energy expansions [10] have contributed substantially to giving a global understanding of these phenomena, resulting from the interplay between electronic interactions, electron–phonon couplings and thermal excitations. In some of these models, the charge-transfer variation $\Delta\rho$ has been considered as a leading parameter in governing the transition from the high-symmetry (HS) phase to the low-symmetry (LS) phase. Its value is currently extracted from optical and diffraction experiments. Due to the complexity of the crystalline structure, no attempt has been made to obtain a direct estimate of this quantity by means of electronic and total-energy calculations.

The method used in this paper is the PAW method [11] within the gradient-corrected local density approximation (LDA) [12], which allows straightforward atomic relaxations and can be applied either to the whole crystal or to isolated neutral or charged molecules, dimers, fragments, ..., thus providing the means to determine *ab initio* values for a coherent set of parameters for model Hamiltonians. This method does not treat very well the Van der Waals interactions, which are known to be non-negligible for these molecular compounds. However, their variations at the transition are expected to be rather small. Moreover, we are not here studying the relative stabilities of the crystalline phases or the mechanism of the transition. Our aim is twofold. First we want to get from three-dimensional (3D) *ab initio* calculations a microscopic description at an atomic scale of the electronic distribution in the crystal and extract a quantitative estimate of the parts played respectively by the lattice contraction (totally symmetric) and the loss of inversion symmetry in the crystal (symmetry breaking) in the CT variation at the N–I transition. Secondly, these calculations provide a good way to check the validity of the assumption of 1D character currently made for the main quantum interactions in these structures.

From the numerical point of view, TTF-2, $5Cl_2BQ$ has, over TTF-CA, the advantage that its crystalline structure has only one D–A pair per unit cell instead of two. Its crystalline structure is first presented in section 2. In section 3, we show how the electronic structure and its redistribution in the LS phase can be qualitatively described in a simple 1D scheme based on symmetry considerations, in the framework of which we introduce the principal intra-chain hopping integral t. In section 4, we present a complete analysis of the valence and conduction electronic states by means of 3D calculations for the HS phase and a relaxed LS phase. These calculations lead to a clear visualization of the connection between symmetry breaking and CT variation. In section 5, we analyse the intra- and inter-chain quantum interactions in the valence (VB) and conduction bands (CB), and estimate the CT variation within a 3D tight-binding model fitted to the *ab initio* results. In the last section, we discuss to what extent the global CT from D to A can be extracted from a representation of the crystal as 1D linear chains of alternating donor and acceptor molecules. We discuss also the importance of the 3D inter-chain interactions in the different types of N–I phase transition. This is a first step toward the general description of the compounds of the TTF-p-benzoquinone series, which form mixed stacks with very different inter-chain configurations.

2. Crystalline structure

In the experimental structure at ambient temperature and pressure (the HS phase) [5], the D and A molecules are equally spaced along the stacking axis $\boldsymbol{b}$ and each one is located at an inversion centre. The molecular planes are not normal to the axis, but are tilted at an angle of about 24° (figure 1).

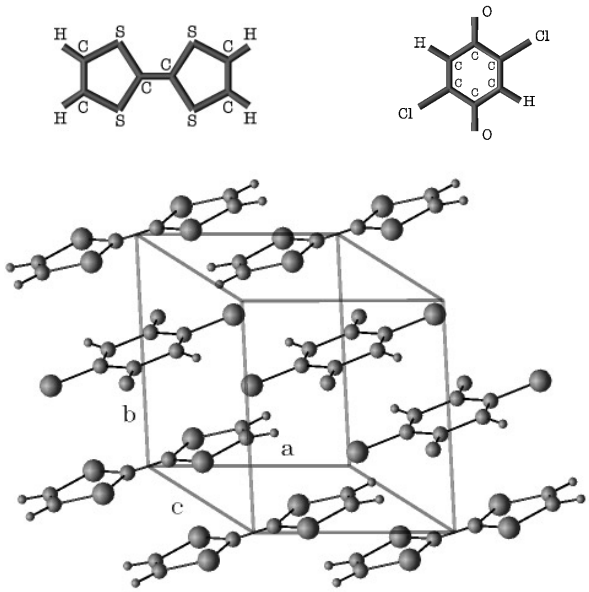

Figure 1. The crystalline structure of TTF-2, 5Cl$_2$BQ: TTF at the corners of the unit cell, 2, 5Cl$_2$BQ, at $\boldsymbol{b}/2$ (the biggest spheres are the Cl atoms). For clarity, some molecules have been omitted. Insets: TTF and 2, 5Cl$_2$BQ backbones.

No crystallographic studies of the low-symmetry phase have been reported up to now. So, we cannot analyse the actual electronic redistribution in this phase. However, when relaxing the atomic positions in the fixed room temperature unit cell, we obtain by total-energy minimization an equilibrium configuration of pairs of slightly deformed molecules along the stacking axis, presented in figure 2. The global deformation of these pairs can be described as a dimerization and an intra-molecular distortion. The dimerization is characterized by a small variation $\boldsymbol{u}$ along the stacks of the vector connecting the centres of mass of the two molecules. Here $\boldsymbol{u}$ is of the order of 0.09 Å (2.54% contraction), which is comparable to the dimerization (2.47%) observed in the low-symmetry structure (40 K) of TTF-CA [3]. The molecules are no longer inversion symmetric: the variation of the bond lengths is typically less than 0.04 Å (4%), and the angular variations less than one degree. The geometry of a TTF molecule versus ionicity in different environments has been extensively explored by experimental [13] as well as theoretical [14] techniques. The bond-length variations in our relaxed configuration (increase of the length of the central C–C bridge, decrease of the mean distance between these C atoms and their S neighbours, ...) is consistent with an increase of the charge on the TTF molecule, i.e. an increase of the electron transfer from D to A. As can be seen in figure 2, some atoms are nearly not displaced in the relaxation, especially in the flexible TTF molecule. The resulting distortions are hence characterized by opposite curvatures of the two molecules of a given pair.

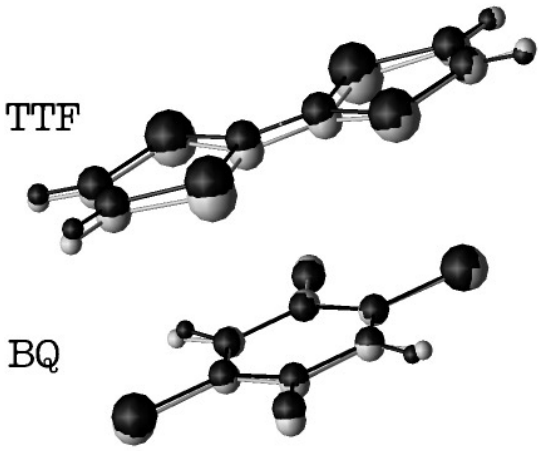

Figure 2. Deformation of a TTF-2, $5Cl_2BQ$ pair along a chain in the relaxed structure (white), compared to the HS configuration (black).

In this artificial structure, which we shall call the 'relaxed LS phase' (RLS), the molecular conformation should be similar to the one adopted in the actual LS phase. As it has been obtained numerically by relaxing the constraint of inversion symmetry in a fixed unit cell, its comparison to the HS phase in the same unit cell gives an order of magnitude for the part of the CT variation that can be expected from the loss of inversion symmetry at the actual transition.

3. Symmetry and the 1D model

The D and A molecules are the elementary entities in these materials. The quantitative knowledge of the electronic properties of the isolated molecules [14, 15] is the starting point for the analysis of the electronic redistribution in the crystal. It is well known that the molecular orbitals principally involved in this charge redistribution, i.e. the lowest unoccupied molecular orbital (LUMO) of the acceptor A and the highest occupied molecular orbital (HOMO) of TTF, are formed from linear combinations of p atomic orbitals pointing perpendicularly to the molecular planes and coupled by π-interactions. Moreover, the HOMO of TTF is inversion antisymmetric, whereas the LUMO of A is inversion symmetric.

Due to this symmetry difference, no quantum mixing of these molecular states is possible at the centre Γ of the Brillouin zone (BZ) in the HS phase. The maximum dispersion is therefore expected at the border $Y = \boldsymbol{b}^*/2$ of the BZ and not at Γ as in polyacetylene. This has been demonstrated by our preliminary 1D *ab initio* calculations [16]. There are two immediate consequences of this. First, a self-consistent calculation limited to one $\boldsymbol{k}$-point at Γ, which is sometimes used for complex systems with many atoms per unit cell, leads in this case to qualitatively wrong results: in the absence of hybridizations the only possible solutions are those acceptable for isolated molecules, i.e. a CT of $0e^-$, $1e^-$ or $2e^-$. Secondly, for model Hamiltonians, it is incorrect to consider only one hopping integral t along the chain, as has been supposed acceptable up to now [9]. In the HS phase, the inversion centre imposes the restriction that the two hopping integrals from D to A and A to D along the chain are opposite. For analytical convenience, we define the absolute value of these integrals as $t = \theta/2$:

$$\begin{aligned} &\langle 0, \mathrm{D}|H|0, \mathrm{D}\rangle = E^0_{\mathrm{D}} \qquad && \langle b/2, \mathrm{A}|H|b/2, \mathrm{A}\rangle = E^0_{\mathrm{A}} \\ &\langle 0, \mathrm{D}|H|b/2, \mathrm{A}\rangle = -\theta/2 \qquad && \langle -b/2, \mathrm{A}|H|0, \mathrm{D}\rangle = \theta/2. \end{aligned} \tag{1}$$

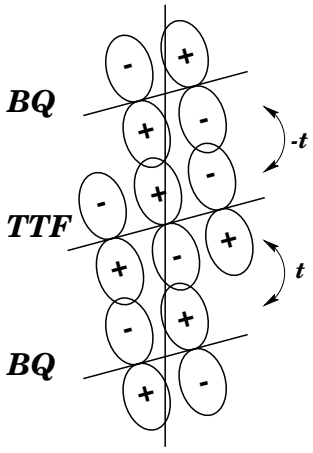

Figure 3. A schematic representation of the electronic intra-chain contacts in the valence band. Each point represents an atom or a group of atoms: S–(C–C)–S for TTF, (C–C–C)–(C–C–C) for 2, 5Cl$_2$BQ.

where $|0, \mathrm{D}\rangle$ represents the HOMO of donor D and $|b/2, \mathrm{A}\rangle$ the LUMO of acceptor A in the unit cell. We have already shown that these inter-molecular contacts are in fact quantum interactions between specific atoms of the two molecules [16], which act essentially perpendicularly to the molecules. These interactions are schematically represented in figure 3, where each point represents an atom or a group of atoms connected by bonding interactions: the two C–C–C triplets of 2, 5Cl$_2$BQ, the central C–C bond and two opposite sulphur atoms on TTF (which are those with the longest bond length with the central C–C).

In this simple model, the small atomic displacements in the LS phase are interpreted as a 'dimerization' in D–A pairs, which is represented by a global variation u of the inter-molecular distance, similar to the one defined in the previous section. Then the new hopping integrals are decreasing functions of u:

$$\theta\left(\frac{b}{2}+u\right)=\left[\theta\left(\frac{b}{2}\right)+\frac{u^2}{2}\frac{\partial^2\theta}{\partial u^2}\bigg|_{(u=0)}\right]+u\frac{\partial\theta}{\partial u}\bigg|_{(u=0)}=\theta'-\epsilon \tag{2}$$

where ϵ is positive, for the inter-pair interaction, and similarly

$$-\theta\left(\frac{b}{2}-u\right)=-\theta'-\epsilon \tag{3}$$

for the intra-pair interaction. So, the molecular distortion introduces to first order an additional hopping term $-\epsilon$ in the chain, which acts in the same way from D to A and A to D, and hence induces (as in polyacetylene) an additional hybridization at the centre of the BZ [17]. This is the origin of the CT increase due to the loss of inversion symmetry.

4. *Ab initio* 3D calculations

In order to analyse the electronic redistribution due to the loss of inversion symmetry, we performed 3D *ab initio* calculations for the experimental lattice, with flat or relaxed molecules. The calculations were carried out with twelve $\boldsymbol{k}$-points: the eight corners of a reduced part of the Brillouin zone (RBZ) built on $\boldsymbol{a}^*/2$, $\boldsymbol{b}^*/2$ and $\boldsymbol{c}^*/2$, and four extra points with $k_y=\boldsymbol{b}^*/4$ along the edges of the RBZ, obtained by doubling the unit cell in the $\boldsymbol{b}$-direction.

No magnetic properties have been reported up to now for this compound, and our stable configuration is not spin polarized. The corresponding dispersion curves for the VB and CB are displayed in figure 4, where the directions in $\boldsymbol{k}$-space are classified in such a way that the two planes $\Gamma(0, 0, 0)$–$Z(0, 0, 1/2)$–$S(1/2, 0, 1/2)$–$X(1/2, 0, 0)$ and $Y(0, 1/2, 0)$–$U(0, 1/2, 1/2)$–$T(1/2, 1/2, 1/2)$–$W(1/2, 1/2, 0)$ perpendicular to the chain direction are on both sides of Γ–Y. There are small dispersions in these planes, which result from inter-chain 3D contacts. All other bands are typically more than 1 eV away from these bands.

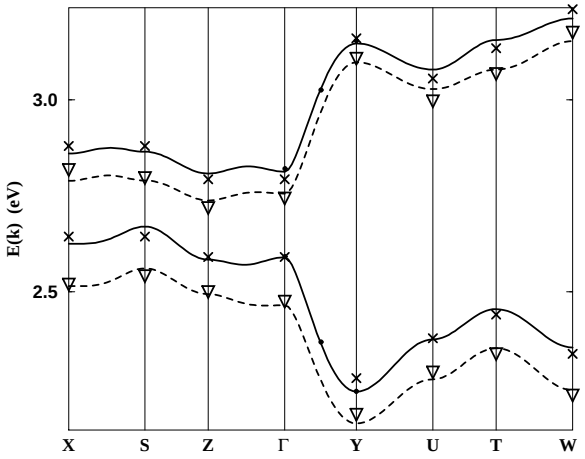

Figure 4. Valence and conductivity bands of TTF-2, $5Cl_2BQ$ in the HS and LS phases. The solid curves (HS) and broken curves (LS) are derived from models (b) and (c). Crosses and triangles are approximate values calculated respectively with models (b′) and (c′).

This compound is a semiconductor with a small and most probably indirect gap: $E_g \simeq 0.14$ eV in the HS phase and $\simeq 0.18$ eV in the LS phase. This value is a lower estimate, in view of the fact that the LDA used in our calculations is known to underestimate the gap of semiconductors (typically by a factor of 2 for polymers [18]). This is consistent with the fact that a non-negligible absorption has been detected in TTF-2, $5Cl_2BQ$ by optical measurements [1] down to 0.5 eV.

The dispersion curves in the RLS phase are very similar to those of the HS phase, except for a global downward shift which explains why we find this phase by energy minimization. It is hence evident that the consideration of just these curves cannot lead to an estimate of the CT variation, which is generally defined as a global electron migration from the donor to the acceptor molecules. We have already shown [16, 17] that the VB electronic distribution in this nearly 1D system appears as a somewhat delocalized cloud along the chains. In that context, the ionicity ρ of each molecule is not a well defined quantity in the crystal, and is not a direct by-product of our *ab initio* calculations. In order to estimate the contribution of the VB to the charge on each molecule, we proceed in the following way. Neglecting the weak hybridization of the VB and CB with other electronic states in the crystal, the VB Bloch function in the HS or RLS phase is assumed to be a linear combination of Bloch functions built with the HOMO of TTF and the LUMO of 2, $5Cl_2BQ$:

$$|\Psi_k\rangle = C_{\mathrm{D}}^k \left[\sum_n \mathrm{e}^{\mathrm{i}\boldsymbol{k}\cdot\boldsymbol{R}_n} |\boldsymbol{R}_n, \mathrm{D}\rangle \right] + C_{\mathrm{A}}^k \left[\sum_n \mathrm{e}^{\mathrm{i}\boldsymbol{k}\cdot\boldsymbol{R}_n} |\boldsymbol{\tau}_n, \mathrm{A}\rangle \right]. \tag{4}$$

Here, the molecular orbitals $|\mathrm{D}\rangle$ and $|\mathrm{A}\rangle$ are calculated using *ab initio* simulations for isolated

molecules in their symmetrical or distorted geometry; $\boldsymbol{R}_n$ represents a primitive translation and $\boldsymbol{\tau}_n$ a translation $\boldsymbol{R}_n + \boldsymbol{b}/2$. At the Γ point the valence state in the HS phase is a pure TTF state [16, 17]: $|C_{\rm A}^{\Gamma}|^2 = 0$. For a given phase, the CT ρ_{VB} from TTF to 2, 5Cl$_2$BQ in the VB is due to the hybridization between the two Bloch functions and is thus given by the mean value of the weight $|C_{\rm A}^{k}|^2$ of the acceptor in this band. This weight can be considered as a parameter, which is obtained for each $\boldsymbol{k}$-point by mean square minimization in the unit cell of the difference between equation (4) and the *ab initio* value of the total Bloch function. Figure 5 displays these weights at the eight corners of the RBZ for the HS and RLS phases. It shows that the CT increase in the RLS phase results mainly from an additional hybridization throughout the whole Γ–Z–S–X plane in $\boldsymbol{k}$-space, which is no longer forbidden by symmetry. It corresponds to a pairing of the D and A electronic states by deformation of the total Bloch function, related to the small 'geometric' pairing in real space due to the deformation of the molecules (figure 2).

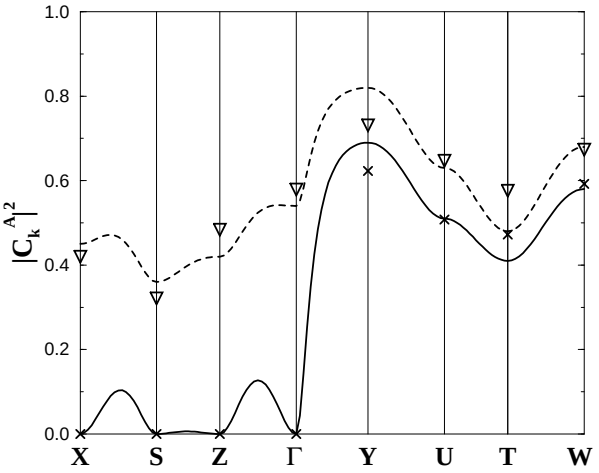

Figure 5. The weight of the A molecule in the Bloch function of the VB, as derived from equation (4), for the HS (solid curve) and LS (broken curve) phases. The crosses and triangles have the same meaning as for figure 4.

5. Inter-molecular contacts and charge transfer

We now express these global *ab initio* results in terms of a tight-binding scheme, which allows us to estimate the relative strengths of the different quantum inter-molecular interactions and get a quantitative value of the CT variation. We first define nearest-neighbour inter- or intra-chain contacts:

$$\begin{aligned} &\langle \boldsymbol{b}/2, \mathrm{A}|H|\boldsymbol{\tau}_i, \mathrm{A}\rangle = \gamma_i/2 \qquad && \langle \boldsymbol{0}, \mathrm{D}|H|\boldsymbol{R}_i, \mathrm{D}\rangle = \beta_i/2 \\ &\langle \boldsymbol{0}, \mathrm{D}|H|\boldsymbol{\tau}_j, \mathrm{A}\rangle = -\theta_j/2 - \epsilon_j/2 \qquad && \langle -\boldsymbol{\tau}_j, \mathrm{A}|H|\boldsymbol{0}, \mathrm{D}\rangle = \theta_j/2 - \epsilon_j/2 \end{aligned} \tag{5}$$

where ϵ_j appears due to the deformations of the molecules in the LS phase, which are no longer supposed to be rigid displacements. These interactions introduce a slight dispersion of the on-site energies:

$$\begin{aligned} E_{\rm A} &= E_{\rm A}^0 + \sum_i \gamma_i \cos \boldsymbol{k}\cdot\boldsymbol{R}_i \\ E_{\rm D} &= E_{\rm D}^0 + \sum_i \beta_i \cos \boldsymbol{k}\cdot\boldsymbol{R}_i. \end{aligned} \tag{6}$$

Defining the quantities:

$$\delta = E_{\mathrm{A}} - E_{\mathrm{D}} \qquad \sigma = E_{\mathrm{A}} + E_{\mathrm{D}}$$
$$\Delta_\theta = \sum_j \theta_j \sin \boldsymbol{k}\cdot\boldsymbol{\tau}_j \qquad \Delta_\epsilon = \sum_j \epsilon_j \cos \boldsymbol{k}\cdot\boldsymbol{\tau}_j \tag{7}$$

one gets a system of non-linear equations for the energies:

$$E^k_\pm = \frac{\sigma}{2} \pm \frac{1}{2}\sqrt{\delta^2 + 4\Delta^2_\theta + 4\Delta^2_\epsilon} \tag{8}$$

together with the corresponding weights of A in the VB:

$$|C^k_{\mathrm{A}}|^2 = 1 - \frac{\delta}{\sqrt{\delta^2 + 4\Delta^2_\theta + 4\Delta^2_\epsilon}} \qquad \text{(two spins)}. \tag{9}$$

We consider now the eight corners of the RBZ, and take as input in (8) and (9) the *ab initio* energies of figure 4 and the weights of figure 5. This in fact introduces the approximation on the weights inherent to equation (9), but leads to a simple determination of a set of parameters giving the 'exact' values at the corners of RBZ for the HS phase (model a) and the RLS phase (model b with $\Delta_\epsilon \neq 0$). These models have been used to plot the curves in figures 4 and 5. It must be noted that they are not directly comparable to model Hamiltonians developed in the literature. First the *ab initio* energies used in the fit are affected by weak hybridizations with other bands. Secondly, they include the effect on the VB of its coupling to the total electron density in the crystal via Coulomb and exchange–correlation interactions, whereas these interactions are limited to the VB density in model Hamiltonians and represented by extra Madelung and Hubbard terms between point charges. Though these effects are not explicitly taken into account in our models, they are implicitly included in the values of our parameters, via the fit to the *ab initio* energies.

In order to build simplified models (a′ and b′), one retains the largest of these parameters (table 1). These models lead to approximate values for the energies and weights, also indicated in figures 4 and 5, which are in reasonable global agreement with the *ab initio* results. We have thus determined the most important intra- and inter-molecular interactions in the VB and CB electronic states.

Table 1. Values (in eV) of the principal parameters of the tight-binding fits. First column: inter-molecular vectors. Second column: corresponding parameters. Columns 3 and 4: 3D fits for the HS (a′) and RLS (b′) phases. Columns 5 and 6: strictly 1D a_1 and b_1 fits extracted from 3D *ab initio* calculations.

Vector	Parameter	a′ (HS)	b′ (RLS)	a_1 (HS)	b_1 (RLS)
0	$E^0_{\mathrm{A}} - E^0_{\mathrm{D}}$	0.28	0.21	0.25	0.15
$\boldsymbol{a}$	γ	−0.04	−0.04	0	0
	β	−0.03	−0.02	0	0
$\boldsymbol{b}$	γ'	−0.05	−0.05	−0.01	−0.02
	β'	0.02	0.02	0.02	0.00
$\boldsymbol{b}/2$	θ	0.35	0.39	0.43	0.46
	ϵ	0	0.11	0	0.13
$\boldsymbol{c}+\boldsymbol{b}/2$	θ_τ	0.06	0.06	0	0
	ϵ_τ	0	0.01	0	0

Even in the RLS phase, the on-site energy E_A^0 of the LUMO of the acceptor lies above the energy E_D^0 of the HOMO of the donor: the CT increase does not result from the inversion of these molecular levels. The decrease of $\delta^0 = E_A^0 - E_D^0$ in the RLS phase is the expected effect of an increase of the CT: in a Madelung formulation, it lowers the energy of negatively charged sites (A), and raises that of positively charged sites (D).

Concerning the hopping integrals, our *ab initio* calculations are able to determine the nature of the individual atomic orbitals involved in these contacts from the profile of the iso-density curves of the VB charge distribution for each $\boldsymbol{k}$-point. Beside the intra-chain D–A interaction described by $\pm\theta$ and already shown in reference [16] and figure 3, there is another non-negligible D–A inter-chain contact along the vector $\boldsymbol{\tau} = \boldsymbol{c} + \boldsymbol{b}/2$. This interaction is mainly constituted with S–C contacts. The corresponding hopping integral θ_τ is responsible for the small bumps in $|C_A^k|^2$ along the Γ–Z and S–X directions in the HS phase (figure 5), which are smoothed out in the LS phase due to the combined action of θ_τ and ϵ_τ.

Intra-chain second-nearest-neighbour D–D and A–A interactions are important in this structure. They are of the same order of magnitude as the main inter-chain contacts between two donors or two acceptors separated by $\boldsymbol{a}$. These latter interactions are due to couples of (C–C)–S interactions between two D molecules (figure 6(a)) and couples of Cl–O interactions between two A molecules (figure 6(b)). However, due to the large size of the molecules and to the specific atomic character of these interactions, their actual direction is not $\boldsymbol{a}$. They act more or less perpendicularly to the molecules, i.e. in the same direction as the intra-chain couplings sketched in figure 3. Figure 6(a) also reveals weaker S–S interactions between two TTF molecules separated by $\boldsymbol{c}$, which are taken into account in models a and b, but neglected in the simplified ones.

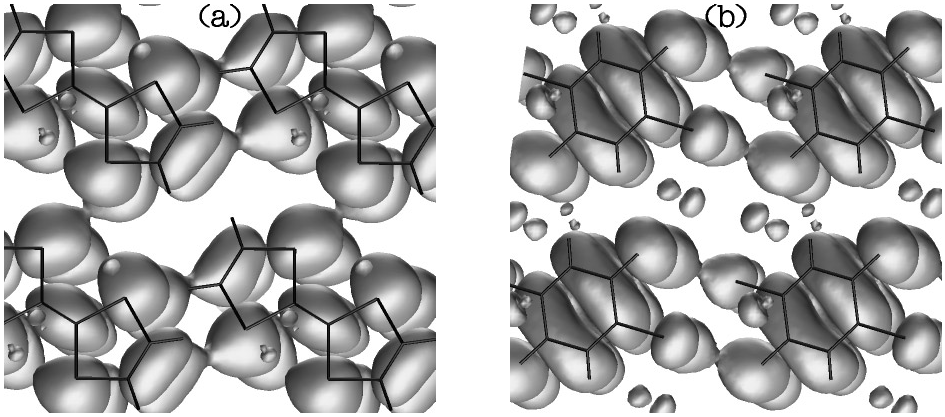

Figure 6. Iso-density representations of the electronic states at $\boldsymbol{k}$ = Z ($\boldsymbol{a}$ horizontal and $\boldsymbol{c}$ nearly vertical), (a) for the VB, displaying D–D inter-chain contacts, and (b) for the CB, displaying A–A inter-chain contacts.

In order to test the relative importance of the intra- and inter-chain hopping integrals in the estimate of the CT variation in the VB, which is the first step toward the building of valid model Hamiltonians for this class of compounds, these models are now further simplified by suppressing all inter-chain hopping integrals. There are two ways to get 1D models. Either (models a″ and b″) one retains only the intra-chain interactions ($\boldsymbol{0}$, $\boldsymbol{b}$ and $\boldsymbol{b}/2$ in table 1) in the previous 3D models, which amounts to replacing the energies and the weights in the two planes Γ–Z–S–X and Y–U–T–W by constant mean values. This procedure averages the

3D effects perpendicular to $\boldsymbol{b}^*$. Or one determines effective intra-chain parameters by a fit just based on Γ and Y (models a_1 and b_1, table 1). In this case, the energies and weights in the two $\boldsymbol{k}$-planes are those of Γ and Y. The parameters for these two procedures are slightly different, with a higher value of θ in the latter, which is in good agreement with previously estimated values [5] of $t = \theta/2 \simeq 0.2$ eV. In all models, ϵ is of the order of 0.1 eV, i.e. 1/4 of θ.

Values of ρ_{VB} for the HS phase, calculated from (9) as the mean value of $|C_A^k|^2$ in the VB, are given in table 2 for the full or simplified fits. As it is but weakly affected by the progressive reduction of the number of inter-chain parameters, this CT is essentially due to θ along the chains [19]. It is rather high compared to the estimated CT obtained by vibrational spectra [5] ($\rho \leqslant 0.2e^-$). But first of all, as mentioned above, the ionicity of the molecules in a system presenting a partially delocalized electronic distribution is not a uniquely defined quantity. The total CT extracted from experiments may be different from its theoretical value deduced from equations of type (4) or from Mulliken's overlap population techniques. Secondly, our LDA calculations probably underestimate the gap and hence overestimate the hybridization between the VB and CB. Thirdly, our estimate has been obtained from equation (4), which describes the charge transfer in an isolated two-band system. The global charge transfer (all bands included) may be different, due to an electronic redistribution in lower bands.

Table 2. Charge transfer in the valence band and its variation from the HS to the RLS phase, as obtained from the different models. x, x′, x″, x_1: increasing degree of simplification of the models (x = a or b).

Model	a (HS)	b (RLS)	$\Delta\rho_{VB}$
x	0.49	0.67	0.18
x′	0.46	0.64	0.18
x″	0.42	0.61	0.19
x_1	0.52	0.74	0.22

The CT variation is probably less sensitive to the definition of the molecular charge, and is therefore a physically more interesting quantity. The CT variation $\Delta\rho_{VB}$ from the HS to the RLS phase in a fixed lattice, also given in table 2, is mainly due to the introduction of ϵ (first-order effect), and an increase of θ (second-order effect). It is about $0.18e^-$, when estimated from parameters extracted from 3D calculations. In 1D models, the CT and its variation ($0.22e^-$) are slightly higher. To get a feeling for the relative importance of this variation, these values should be compared to the total CT variation from low to high pressure in TTF-2, $5Cl_2BQ$ [5]: $\Delta\rho \simeq 0.6e^-$, or to the CT discontinuity in TTF-CA [2, 20]: $\Delta\rho \leqslant 0.4e^-$, values which both include lattice contraction effects which have not been considered in our calculations. This shows that the sole symmetry breaking, i.e. the weak deformation of the molecules, is responsible for a non-negligible part of the observed CT variation.

These results illustrate one of the very interesting properties of these materials. The CT variation in the VB due to the symmetry breaking is mainly controlled by the interactions along the mixed stacks, thus confirming the nearly 1D character of the electronic distribution in the VB (the lattice contraction due to pressure adds a second contribution to $\Delta\rho$ by increasing the hopping integral θ). On the other hand, the molecular character of the basic entities is responsible for the fact that very small atomic displacements (of the same order of magnitude as in standard ferroelectrics such as perovskites) lead to surprisingly large CT variations in the crystal, due to a cooperative effect of all atoms within the molecular orbitals concerned, though the contribution of each individual atom seems quite small.

6. 1D versus 3D

In most of these mixed-stack organic compounds, the molecules form well defined 'mixed planes' or sheets containing both donors and acceptors pertaining to different stacking chains. These mixed planes are conspicuous in structures such as TMB-TCNQ [21], DMTTF-CA [7] and TTF-2, 5Cl$_2$BQ [5]. They are also visible in TTF-CA [3] but form in that case two intersecting stacks of planes due to the existence of a glide plane connecting the two equivalent D–A pairs in the unit cell. These four compounds undergo N–I transitions, whereas TTF-bromanil (or TTF-BA), which has a very different crystalline configuration, remains strongly ionic even in its high-symmetry phase [22].

In TTF-2, 5Cl$_2$BQ, the mixed planes are defined by the two vectors $\boldsymbol{c}$ and $\boldsymbol{a} + \boldsymbol{b}/2$. Interestingly, none of the main inter-molecular contacts determined above in the VB occur in those planes. In order to understand the origin of these structures and their part in the electronic distribution, we have explored the total electron density (except for inner core states) in real space, given by our *ab initio* calculations. In figure 7(a), which represents a section through the iso-density surfaces along one of the mixed planes, several inter-molecular couplings can be seen: (C–H)–O contacts between TTF and 2, 5Cl$_2$BQ molecules separated by $\boldsymbol{a} + \boldsymbol{b}/2$; (C–H)–Cl contacts between TTF and 2, 5Cl$_2$BQ molecules separated by $\boldsymbol{c} + \boldsymbol{a} + \boldsymbol{b}/2$; and S–S

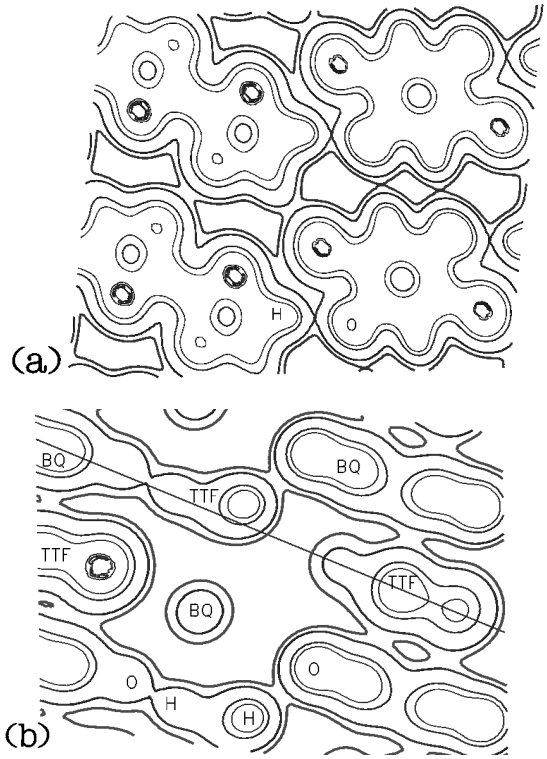

Figure 7. Iso-density representation of the total electron density (except for inner core states): (a) in a mixed plane ($\boldsymbol{a} + \boldsymbol{b}/2$ horizontal and $\boldsymbol{c}$ nearly vertical); (b) in a plane parallel to the chains ($\boldsymbol{b}$ vertical) and to an O–O pair of A molecules (denoted BQ). The straight line in (b) is the trace of the mixed plane considered in (a). The contributions of three chains can be seen in (b): two in front on both sides and one behind, in the middle.

contacts between nearest-neighbour TTF molecules in the $\boldsymbol{c}$-direction. Figure 7(b) represents the total density in a section parallel to the chains and to the O–O direction of a 2, $5Cl_2BQ$ molecule, i.e. nearly perpendicular to this molecule. In this figure, three interactions appear together: the above-mentioned (C–H)–O in-plane D–A interaction, D–A intra-chain contacts and D–A inter-chain contacts in the $\boldsymbol{c} + \boldsymbol{b}/2$ direction, which are again (C–H)–O interactions, distinct from the D–A inter-chain contact already found in the VB and described by θ_τ. By displacing the two sections considered in figure 7, we have verified that the in-plane (C–H)–O interactions are stronger than the intra-chain ones. Thus, beyond the usually considered 1D picture, along the chains, the total electronic structure is described in a more precise way by stacks of parallel molecular sheets connected by weaker interactions perpendicular to these sheets. Similar contacts forming stacks of sheets can also be found in organic conductors [23].

The VB electron density is built from linear combinations of p atomic orbitals perpendicular to the molecules. It thus makes nearly no contribution to the total density in the mixed planes. The intra-plane molecular contacts such as (C–H)–O or S–S result mostly from lower-lying molecular orbitals which are partially delocalized between D and A and hence may play a part in the definition of ρ. Moreover, this electronic distribution in lower bands can also be affected by the loss of inversion symmetry and the lattice contraction. Due to the softness and polarizability of the molecular orbitals, the electronic redistributions in the different bands are necessarily coupled, at least via their effect on the self-consistent electronic potential, so these lower-lying quantum contacts play a key role both in the formation of the crystalline structure and in the global CT variation. The importance of hydrogen bonding in these molecular crystals has of course been known of for a long time. In TTF-CA for example, the two-dimensional (2D) nature of the (C–H)–O network and its role in the lattice contraction parallel and perpendicular to the chains have already been underlined by Batail *et al* [24], and investigated by neutron diffraction experiments [3]. What self-consistent calculations provide in this case, where the lattice contraction and the molecular distortions are known, is a way to get a quantitative estimate of the contribution of the quantum inter-chain interactions to the structural phase transformation.

A first idea of the part played by these interactions in the observed differences in the N–I transitions can be obtained by inspection of the crystalline structures of TTF-CA, TTF-2, $5Cl_2BQ$ and DMTTF-CA. To be comparable, these structures must first be oriented in a coherent way, based on the nature of the contacts. The mixed chains are along $\boldsymbol{a}$ in TTF-CA, $\boldsymbol{b}$ in TTF-2, $5Cl_2BQ$ and $\boldsymbol{c}$ in DMTTF-CA [25]. This provides a first lattice parameter which we call $\boldsymbol{a}_1$, whatever its standard name. Next, it must be noted that a strong coupling exists in the three compounds between neighbouring chains, separated by $\boldsymbol{a}_2 = \boldsymbol{b}$ in TTF-CA and by $\boldsymbol{a}_2 = \boldsymbol{a}$ in both TTF-2, $5Cl_2BQ$ and DMTTF-CA. The similarity of the chain configurations in the $\boldsymbol{a}_2$-direction in the three compounds becomes striking when one superposes the projections of the atomic positions perpendicular to the chains: the three pictures are nearly identical (figure 8). On the other hand, the three compounds are completely different when one compares the positions of the chains in the third direction: $\boldsymbol{a}_3 = \boldsymbol{c}$ in TTF-CA and TTF-2, $5Cl_2BQ$, and $\boldsymbol{a}_3 = \boldsymbol{b}$ in DMTTF-CA, due to the large difference in the absolute value of this parameter. In DMTTF-CA, the inter-chain distance in this direction is larger than in TTF-2, $5Cl_2BQ$, due to the steric hindrance induced by the presence of the methyls. Hence, the S–S coupling between D molecules separated by $\boldsymbol{a}_3$ detected in TTF-2, $5Cl_2BQ$ must be much weaker in DMTTF-CA. In TTF-CA, additional chains due to the glide plane are placed in between, which are equivalent but differently oriented. The inter-chain quantum contacts are very different in that case.

This provides simple arguments based on the idea of Coulomb frustration developed by Hubbard and Torrance [26] a long time ago. In the ionic phase of TTF-CA, the nearest

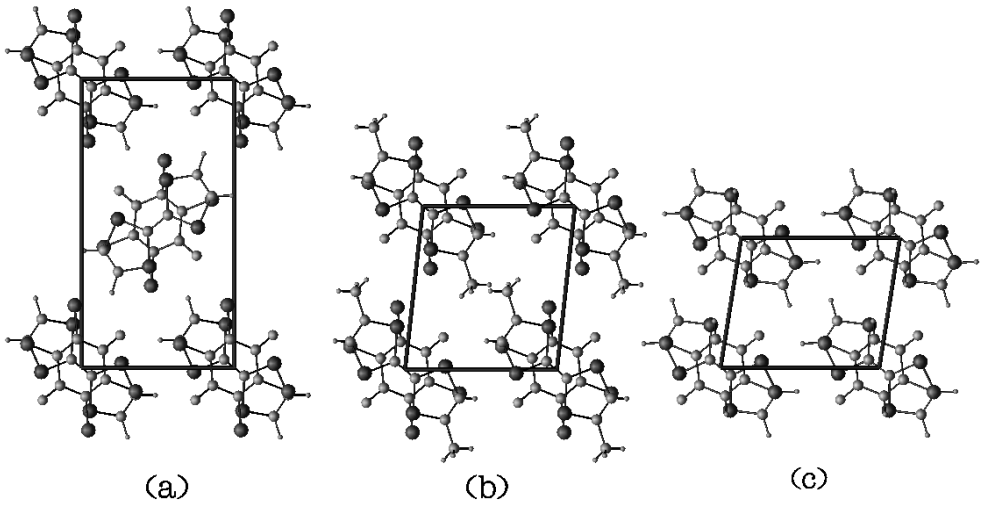

Figure 8. The crystalline structure of (a) TTF-CA, (b) DMTTF-CA and (c) TTF-2, 5Cl$_2$BQ. Projections onto the ($\boldsymbol{a}_2$, $\boldsymbol{a}_3$) plane. $\boldsymbol{a}_2$ is horizontal.

neighbours of a D^+ molecule in the ($\boldsymbol{a}_2$, $\boldsymbol{a}_3$) plane are A^- molecules, which is a favourable situation from the electrostatic point of view, so the transition can be easily obtained by pressure and temperature variations. In TTF-2, 5Cl$_2$BQ or DMTTF-CA, the neighbours of a D^+ molecule in the same plane are also D^+ molecules, which is a less favoured electrostatic configuration. The ionic state in TTF-2, 5Cl$_2$BQ is more difficult to reach, and this can be done only under high pressure. This may be due to a non-negligible quantum coupling between all of the chains in the two directions $\boldsymbol{a}_2$ and $\boldsymbol{a}_3$, imposing the same electronic state for all D and all A molecules. In DMTTF-CA, the inter-stack coupling along $\boldsymbol{a}_3 = \boldsymbol{c}$ is weaker, allowing a possible staging effect in this direction, with alternation of nearly neutral and nearly ionic chains [7], which is of course electrostatically less demanding.

One has hence to be careful when trying to find the driving force of these transitions with model Hamiltonians based as regards their electronic part on the HOMO of D and the LUMO of A. The last occupied and the first empty states have a clear 1D character along the chains, which explains the anisotropic behaviour of the conductivity, optical properties etc. But the global charge-density distribution also results from important inter-chain 3D contacts in lower bands. These quantum interactions have not yet been taken into account in model Hamiltonians. They are not equivalent to the Madelung inter-chain couplings considered up to now, which are by nature classical interactions. Hence, a detailed numerical 3D analysis of the interplay between electronic distributions in the VB and lower bands should be performed for real crystals under pressure in order to test how and to what extent different N–I transitions could be quantitatively described by 'effective' 1D and two-band models.

7. Conclusions

We have shown here that it is now possible to analyse the electronic interactions in complex mixed-stack organic materials by *ab initio* self-consistent numerical techniques. A clear understanding, at a microscopic level, of the quantum intra- and inter-chain interactions in the crystal of TTF-2, 5Cl$_2$BQ has been obtained. For the valence and conduction states, the

contacts are dominantly of 1D character along the stacks, and a tight-binding modelling is possible. Stronger and lower-lying 3D quantum interactions are responsible for the formation of mixed sheets of molecules in the crystalline structure, and may be at the origin of the observed differences in the features of the N–I transition in different compounds. The total charge transfer, or ionicity of the molecules, and its variation result both from the loss of inversion symmetry at the N–I transition and the lattice contraction. We have analysed here the tight relation between symmetry breaking and charge-transfer increase in a fixed unit cell for the VB states, and shown that it constitutes a non-negligible part of the total CT variation in these materials.

Acknowledgments

This work benefited from collaborations within, and has been partially funded by, the Human Capital and Mobility Network on ' Ab initio (from electronic structure) calculation of complex processes in materials' (Contract No ERBCHRXTC930369). Parts of the calculations were supported by the 'Centre National Universitaire Sud de Calcul' (France). We would also like to thank P Blöchl (IBM-Zürich) for his help concerning the use of his PAW program, and many useful discussions.

References

[1] Torrance J B, Vasquez J E, Mayerle J J and Lee V Y 1981 *Phys. Rev. Lett.* **46** 253
[2] Jacobsen C S and Torrance J B 1983 *J. Chem. Phys.* **78** 112
[3] Le Cointe M, Lemée-Cailleau M H, Cailleau H, Toudic B, Toupet L, Heger G, Moussa F, Schweiss P, Kraft K H and Karl N 1995 *Phys. Rev.* B **51** 3374
[4] Lemée-Cailleau M H, Le Cointe M, Cailleau H, Luty T, Moussa F, Roos J, Brinkmann D, Toudic B, Ayache C and Karl N 1997 *Phys. Rev. Lett.* **79** 1690
[5] Girlando A, Painelli A, Pecile C, Calestani G, Rizzoli C and Metzger R M 1993 *J. Chem. Phys.* **98** 7692
[6] Matsuzaki S, Hiejima T and Sano M 1991 *Bull. Chem. Soc. Japan* **64** 2052
[7] Aoki S, Nakayama T and Miura A 1993 *Phys. Rev.* B **48** 626
Nogami Y, Taoda M, Oshima K, Aoki S, Nakayama T and Miura A 1995 *Synth. Met.* **70** 1219
[8] Kikuchi K, Yakushi K and Kuroda H 1982 *Solid State Commun.* **44** 151
Okamoto H, Mitani T, Tokura Y, Koshihara S, Komatsu K, Iwasa Y and Koda T 1991 *Phys. Rev.* B **43** 8224
[9] Nagaosa N 1986 *J. Phys. Soc. Japan* **55** 2754
Horovitz B and Solyom J 1987 *Phys. Rev.* B **35** 7081
Luty T and Kuchta B 1987 *Phys. Rev.* B **35** 8542
Painelli A and Girlando A 1988 *Phys. Rev.* B **37** 5748
Painelli A and Girlando A 1989 *Phys. Rev.* B **39** 9663
Iizuka-Sakano T and Toyozawa Y 1996 *J. Phys. Soc. Japan* **65** 671
[10] Nagaosa N 1986 *J. Phys. Soc. Japan* **55** 3488
Kojyo N and Onodera Y 1987 *J. Phys. Soc. Japan* **56** 3228
Luty T 1996 Relaxations of excited states and photoinduced phase transitions *Proc. 19th. Taniguchi Symp.* ed K Nasu (Berlin: Springer)
[11] Blöchl P 1994 *Phys. Rev* B **50** 17 953
[12] Perdew J P and Zunger A 1981 *Phys. Rev.* B **23** 5048
Perdew J P 1986 *Phys. Rev.* B **33** 8822
Becke A D 1992 *J. Chem. Phys.* **96** 2155
[13] Umland T C, Allie S, Kuhlman T and Coppens P 1988 *J. Phys. Chem.* **92** 6456
[14] Katan C 1999 *J. Phys. Chem.* A at press
[15] Katan C, Blöchl P, Margl P and Koenig C 1996 *Phys. Rev.* B **53** 12 112
[16] Katan C, Koenig C and Blöchl P E 1997 *Solid State Commun.* **102** 589
[17] Katan C, Koenig C and Blöchl P E 1998 *Comput. Mater. Sci.* **10** 325
[18] Springborg M 1993 *Int. Rev. Phys. Chem.* **12** 241

[19] The difference between the parameters of a_1 and b_1 and those extracted from previous *ab initio* calculations limited to three $\boldsymbol{k}$-points along Γ–Y [17] is quite negligible and mainly due to the better estimation of the weights in the present work. This, and other numerical tests, proves that to get a stable value for the gap and charge transfer, it is fundamental to consider at least these three $\boldsymbol{k}$-points. For a quantitative estimate of the 3D effects, more $\boldsymbol{k}$-points in RBZ are needed.

[20] Tokura Y, Okamoto H, Koda T, Mitani T and Saito G 1986 *Solid State Commun.* **57** 607
Hanfland M, Brillante A, Girlando A and Syassen K 1988 *Phys. Rev.* B **38** 1456
Le Cointe M 1994 *PhD Thesis* University Rennes 1, France
At the transition pressure P_c under pressure variation in TTF-CA, the observed charge discontinuity is of about $0.2e^-$ and the lattice contraction is nearly negligible.

[21] Iwasa Y, Koda T, Tokura Y, Kobayashi A, Iwasawa N and Saito G 1990 *Phys. Rev.* B **42** 2374

[22] Girlando A, Pecile C and Torrance J B 1985 *Solid State Commun.* **54** 753

[23] Whangbo M, Williams J M, Schultz A J, Emge T J and Beno M A 1987 *J. Am. Chem. Soc.* **109** 90
Novua J J, Carme Rovira M, Rovira C, Veciana J and Tarres J 1995 *Adv. Mater.* **7** 233

[24] Batail P, LaPlaca S J, Mayerle J J and Torrance J B 1981 *J. Am. Chem. Soc.* **103** 951

[25] TTF-CA [27]: $a = 7.411$ Å, $b = 7.621$ Å, $c = 14.571$ Å, $\beta = 99.1^\circ$.
DMTTF-CA [7]: $a = 7.666$ Å, $b = 8.512$ Å, $c = 7.272$ Å, $\alpha = 103.89^\circ$, $\beta = 91.89^\circ$, $\gamma = 95.91^\circ$.
TTF-2, 5Cl$_2$BQ [5]: $a = 7.935$ Å, $b = 7.216$ Å, $c = 6.844$ Å, $\alpha = 106.9^\circ$, $\beta = 97.58^\circ$, $\gamma = 93.66^\circ$.

[26] Hubbard J and Torrance J B 1981 *Phys. Rev. Lett.* **47** 1750

[27] Mayerle J J, Torrance J B and Crowley J I 1979 *Acta Crystallogr.* B **35** 2988